

The Accuracy of Solar Irradiance Calculations Used in Mesoscale Numerical Weather Prediction

ROBERT J. ZAMORA

NOAA/Environmental Technology Laboratory, Boulder, Colorado

ELLSWORTH G. DUTTON

NOAA/Climate Monitoring and Diagnostics Laboratory, Boulder, Colorado

MICHAEL TRAINER AND STUART A. MCKEEN

NOAA/Aeronomy Laboratory, Boulder, Colorado

JAMES M. WILCZAK

NOAA/Environmental Technology Laboratory, Boulder, Colorado

YU-TAI HOU

NOAA/Environmental Modeling Center, National Centers for Environmental Prediction, Camp Springs, Maryland

(Manuscript received 4 December 2003, in final form 24 August 2004)

ABSTRACT

In this paper, solar irradiance forecasts made by mesoscale numerical weather prediction models are compared with observations taken during three air-quality experiments in various parts of the United States. The authors evaluated the fifth-generation Pennsylvania State University–National Center for Atmospheric Research (PSU–NCAR) Mesoscale Model (MM5) and the National Centers for Environmental Prediction (NCEP) Eta Model. The observations were taken during the 2000 Texas Air Quality Experiment (TexAQS), the 2000 Central California Ozone Study (CCOS), and the New England Air Quality Study (NEAQS) 2002. The accuracy of the model forecast irradiances show a strong dependence on the aerosol optical depth. Model errors on the order of 100 W m^{-2} are possible when the aerosol optical depth exceeds 0.1. For smaller aerosol optical depths, the climatological attenuation used in the models yields solar irradiance estimates that are in good agreement with the observations.

1. Introduction

Elevated surface ozone concentrations (>80 ppb) typically occur during meteorological stagnation events. These events are characterized by weak surface winds, and synoptic-scale subsidence usually associated with high pressure in the lower troposphere (Seaman and Michelson 2000). When synoptic-scale forcing becomes weak, smaller-scale forcing mechanisms drive the observed circulations. The smaller-scale physical processes include land/sea-breeze circulations, slope flows, and differential heating caused by variations in land use.

Representing this smaller-scale forcing in mesoscale forecast models such as the fifth-generation Pennsylvania State University–National Center for Atmospheric Research (PSU–NCAR) Mesoscale Model (MM5; Grell et al. 1994) and the National Centers for Environmental Prediction (NCEP) Eta Model (Black 1994; Janjic 1997; Rogers et al. 1996) places heavy demands on the parameterizations that simulate the surface energy balance. One of the key inputs to the surface energy balance computations is the solar irradiance. Zamora et al. (2003) have shown that an increase of 100 W m^{-2} in the MM5 solar irradiance calculation can lead to significant error in the net radiation forecast by the model. The additional solar radiation increased the net radiation and caused a high bias in the daytime planetary boundary layer (PBL) depths forecast by MM5 during the Nashville, Tennessee, Southern Oxidants Studies (SOS).

Corresponding author address: Robert J. Zamora, NOAA/Environmental Technology Laboratory, R/E/ET7, 325 Broadway, Boulder, CO 80305.
E-mail: Robert.J.Zamora@noaa.gov

Zamora et al. (2003) traced the uncertainty in the predicted solar irradiance over Nashville to an inadequate representation of aerosol and ozone attenuation in MM5. After adding ozone attenuation into the Dudhia (1989, hereafter D89) shortwave solar parameterization and running the model over Boulder, Colorado, where the observed aerosol optical depth (AOD) was 0.125, they found excellent agreement between the observed solar irradiance and the output of the parameterization. Zamora et al. (2003) concluded that accurate solar irradiance estimates could be obtained using the D89 parameterization as long as the AOD remained near 0.1.

Guichard et al. (2003) evaluated the MM5 solar irradiance forecasts for a 2-month period using observations made at the Atmospheric Radiation Measurement (ARM) Program southern Great Plains (SGP) site. They found that differences between the model and the observations varied with averaging period, ranging from 11 to 100 W m^{-2} . Guichard et al. (2003) concluded that aerosols and forecasts of cirrus cloud amount were responsible for the majority of the differences between MM5 and the ARM measurements.

In this paper, we examine the performance of the MM5 D89 solar irradiance parameterization for three elevated surface ozone events that occurred in different regions of the United States during air-quality experimental campaigns. These case studies help us locate regions of the country where aerosol impacts can have an adverse effect on mesoscale numerical model performance. The campaigns included the Texas Air Quality Study 2000 (TexAQS 2000), the Central California Ozone Study (CCOS), and New England Air Quality Study (NEAQS) 2002. We also evaluated the NCEP Eta Model solar irradiance parameterization during the NEAQS 2002 11–16 August elevated surface ozone event.

During each of these experimental campaigns the National Oceanic and Atmospheric Administration (NOAA)/Environmental Technology Laboratory (ETL) in collaboration with the NOAA/Climate Monitoring and Diagnostics Laboratory (CMDL), and the NOAA/Aeronomy Laboratory (AL) made detailed in situ solar and IR radiation observations within the experimental domains near air-chemistry sampling locations. We will show comparisons between the MM5 and the observations suggesting that the MM5 D89 solar irradiance parameterization performed acceptably for the Gulf Coast and Central Valley of California. We will also show differences between the forecast and observed clear-sky irradiances of 80 W m^{-2} for both the NCEP Eta Model and the MM5 along the New England coastal zone during the NEAQS 11–16 August 2002 elevated surface ozone event. The role of AODs exceeding 0.1 during this event will be explored. In this paper we will also assess the impact of the solar irradiance uncertainty on the model forecast skin temperature using analytical methods.

Section 2 of our paper summarizes the observational locations and instruments deployed for each of the elevated surface ozone events. The MM5 model configurations that we used in our studies are presented in section 3. In section 4 we show the comparisons between the forecast and observed solar irradiances. The impact of errors in the model forecast solar radiative fluxes on the model skin temperature forecasts will be explored in section 5. Our summary and conclusions are presented in section 6.

2. Observations

We compared the MM5 solar irradiance forecasts with observations for three case studies. At all three sites, we made broadband solar irradiance measurements at 2.0 m using ventilated (conditioned) Eppley Precision Spectral pyranometers (PSPs). We sampled the pyranometers at 1.0 Hz and averaged the 1.0-Hz samples for 1.0 min. The pyranometers were calibrated at the NOAA/CMDL Solar Calibration Facility. The facility is a World Meteorological Organization (WMO) World Region IV Center. Uncertainty in instantaneous global (2π steradian) solar irradiance measurements made using PSPs arise in two ways: nonideal angular (zenith and azimuth) response of the instrument (Dutton et al. 2001) and thermal offset errors (Philipona 2002). Given these errors we estimate that the broadband solar fluxes are accurate within ± 10 – 15 W m^{-2} .

Our first study event occurred along the Texas Gulf Coast over the Houston/Galveston metropolitan area during the TexAQS 2000 experiment. During the 7-day event that began on 25 August 2000, surface ozone concentrations as high as 199 ppb were observed in the area. The ETL radiative flux observations were located at La Porte, Texas.

The second elevated ozone event occurred over the Central Valley of California during the CCOS 2000 experiment. Surface ozone measurements of 100 ppb were observed during a 4-day period that began on 29 July 2000 near Pleasant Grove, California. The ETL radiative flux measurements were located 7.5 km southeast of Pleasant Grove.

We chose our final study event from a 5-day period beginning on 11 August 2002, where surface ozone measured near Durham, New Hampshire, reached 120 ppb on 3 of the 5 days. The NEAQS 2002 radiative flux measurements were collocated with the University of New Hampshire air-chemistry monitors at Thompson Farm, New Hampshire. In addition to the Eppley PSPs we also deployed a Carter–Scott sun photometer (SP02) at the Thompson Farm location. The SP02 measured AOD at wavelengths of 412, 500, 675, and 862 nm. We sampled the SP02 channels using a single measurement at the start of every minute.

3. Numerical model configurations

All of the MM5 modeling system runs used MM5 version 3.5 in forecast mode using the D89 solar irradiance parameterization. The MM5 and NCEP Eta solar irradiance parameterizations are both essentially based on the Lacis and Hansen (1974) method of computing solar irradiance. The version of Lacis and Hansen (1974) used in the MM5 modeling system does not explicitly account for stratospheric ozone absorption and was tuned using a scattering parameter (XSCA) to the observations obtained during the First International Satellite Land Surface Climatology Project (ISLSCP) Field Experiment (FIFE) (J. Dudhia 2003, personal communication).

Such tuning assumes that all scattering and absorption processes not explicitly included in the parameterization can be represented using a single parameter and that the atmospheric conditions present over the FIFE experimental domain represented typical mean aerosol and ozone optical depths. Thus, stratospheric ozone absorption, aerosol scattering, aerosol absorption, and Rayleigh scattering are all physical processes accounted for in the default tuning of the model.

The ETL TexAQS 2000 MM5 and CCOS 2000 simulations used NCEP Eta boundary and initial conditions and ran for the entire length of the elevated ozone events on a 4-km horizontal grid. Physics choices included the explicit gridpoint moisture scheme, the Eta PBL parameterization, and the Blackadar “slab” land surface model (LSM) (Blackadar 1979; Zhang and Anthes 1982). Our configuration of the model updated the radiative transfer calculations at 10-min intervals. The 4-km simulations of clouds and precipitation relied entirely on the explicit gridpoint moisture scheme and did not employ a convective parameterization.

The NEAQS 2002 MM5 simulations were made by NOAA/Forecast Systems Laboratory (FSL) in real time using the NOAA/FSL Coupled Air Chemistry Modeling System (Grell et al. 2000) running at 27-km horizontal resolution. We used the first 24 h of each FSL MM5 run initialized at 0000 UTC to create a 5-day time series for our radiative flux comparison. All the runs used NCEP Eta boundary conditions and FSL RUC initial conditions. The NOAA/FSL physics choices include the explicit gridpoint moisture scheme, the Grell (1993) convective parameterization, the Burk–Thompson PBL parameterization (Burk and Thompson 1989), and the NOAA/FSL LSM (Smirnova et al. 1997). The FSL MM5 simulations updated the radiative transfer calculations at 30-min intervals.

We also created a time series of gridpoint output using the first 24 h of each 0000 UTC operational 12-km NCEP Eta run and compared the forecast solar irradiances with the Thompson Farm observations during the 11–16 August 2002 elevated ozone event. The NCEP Eta Model calculated the radiation at hourly intervals

using the zenith angle that represented the average zenith angle of the hourly interval.

4. Observational comparisons

The comparison between the MM5 forecast irradiance and the La Porte, Texas, observations during the TexAQS 2000 elevated surface ozone event indicate that, overall, the model produced excessive cloud cover. This cloud cover accounts for the majority of the differences between the model and the observations for the first 6 days of the Houston/Galveston elevated ozone event (Fig. 1). However, from 30 August to 1 September, clearer conditions prevailed in both the model and the observations. During these clearer-sky conditions, the MM5 forecast solar fluxes near solar noon are 34 W m^{-2} higher than the La Porte observations (Fig. 2).

We obtained a similar result when we compared the MM5 forecast solar irradiances with the Pleasant Grove observations (Fig. 3). Once again, clouds are a source of uncertainty, and on 30 July they dominate the comparison. During the two clear-sky periods, we detected a 36.1 W m^{-2} difference between the model and the observations near solar noon.

In both of the previous case studies we find that MM5 overestimates the solar irradiance by about 30 W m^{-2} . Because the default tuning of the MM5 solar irradiance scheme accounts for ozone absorption and aerosol attenuation together we cannot isolate the cause of the discrepancy between the model and the observations without observations of AOD. However, when one considers that a $10\text{--}15 \text{ W m}^{-2}$ low bias can

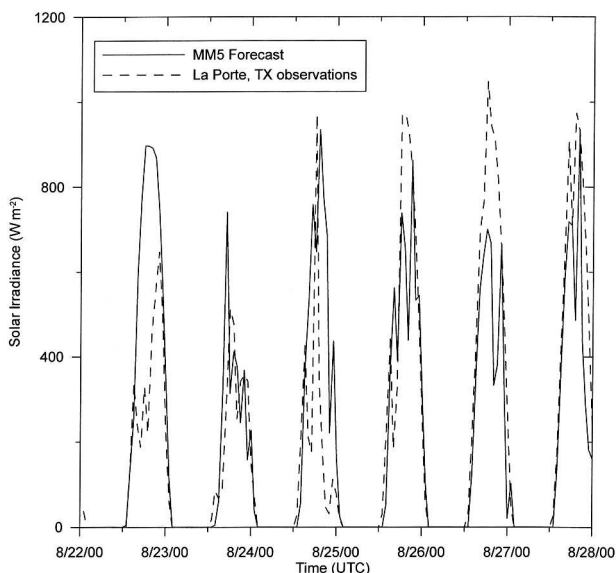


FIG. 1. Solar irradiance predicted by MM5 (solid) and measured (dashed) solar irradiance at La Porte, TX, as a function of time for 22–28 Aug 2000.

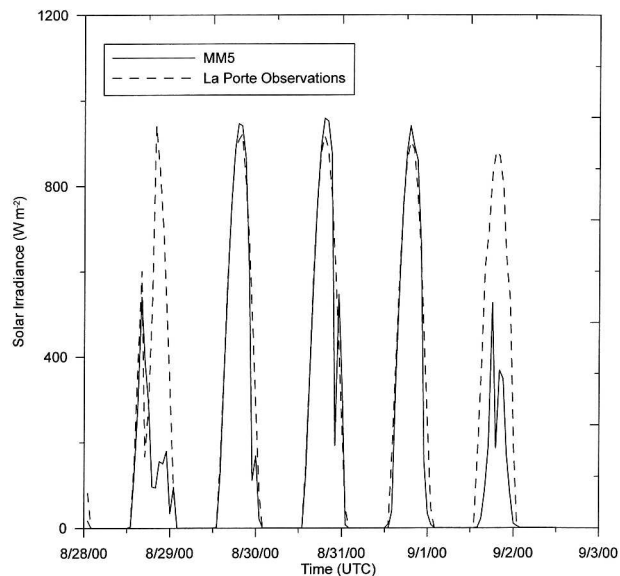


FIG. 2. Solar irradiance predicted by MM5 (solid) and measured (dashed) solar irradiance at La Porte, TX, as a function of time for 28 Aug–2 Sep 2000.

exist in the pyranometer observations, the comparisons suggest that the D89 forecast irradiances are accurate within 3%–4% for the Texas and California case studies.

During the NEAQS 2002 experiment, we compared the radiative flux measurements obtained near Durham, New Hampshire, with both MM5 and the NCEP Eta Model. The MM5 comparison for the 11–16 August 2002 elevated surface ozone event reveals a 10% dis-

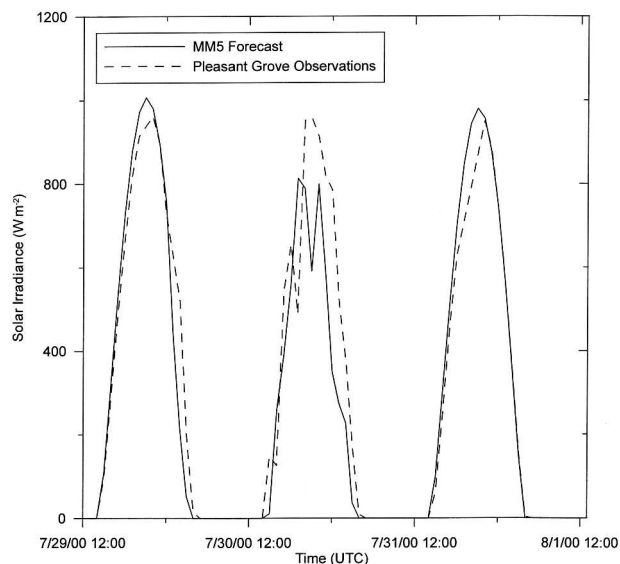


FIG. 3. Solar irradiance predicted by MM5 (solid) and measured (dashed) solar irradiance at Pleasant Grove, CA, as a function of time for 29 Jul–1 Aug 2000.

crepancy between the forecast solar fluxes and the observations at solar noon (Fig. 4). When we plotted the differences between the MM5 fluxes and the observations, we found that the MM5 solar fluxes are $\sim 100 W m^{-2}$ higher than the observations on 4 of the 5 days of the event (Fig. 5), and $80 W m^{-2}$ higher than the observations for all days. Similar results were obtained in the NCEP Eta Model comparison (Fig. 6), where we again found a $\sim 90 W m^{-2}$ difference between the Eta forecast irradiance and the observations on 12–14 August.

The performance of both mesoscale models using a similar radiation parameterization suggests that a fundamental physical process has been underestimated in the radiative transfer routines. When one examines the AOD observations at 500 nm for the event, the role of aerosols becomes clearer. The observations show that AODs exceeded 0.1 on all days of the event, and that the AODs increased from 0.2 to the 0.5–0.7 range at the same time the difference between the models and the observations jumped from 70 to $90 W m^{-2}$ (Fig. 7).

When we examined the observed solar irradiance, AOD, and the Eta Model forecast irradiance for zenith angles of 72° , 61° , 51° , and 41° we found that the observed irradiance showed a strong dependence on AOD (Fig. 8). For every 0.1 increase in AOD, the solar irradiance decreases by $\sim 12 W m^{-2}$. This result is consistent with the findings of Satheesh et al. (1999). At the same time, the slope of the fit to the modeled irradiances as a function of AOD appeared much steeper, indicating insensitivity to the aerosol loading (Fig. 8).

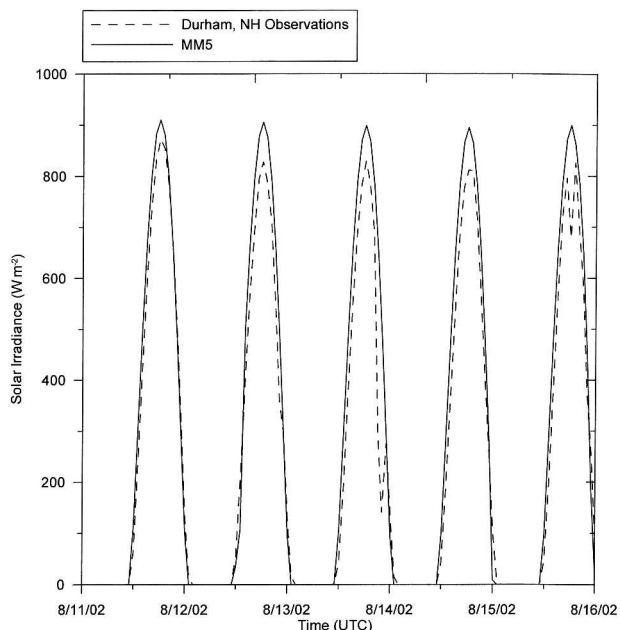


FIG. 4. Solar irradiance predicted by MM5 (solid) and measured (dashed) solar irradiance at Durham, NH, as a function of time for 11–16 Aug 2002.

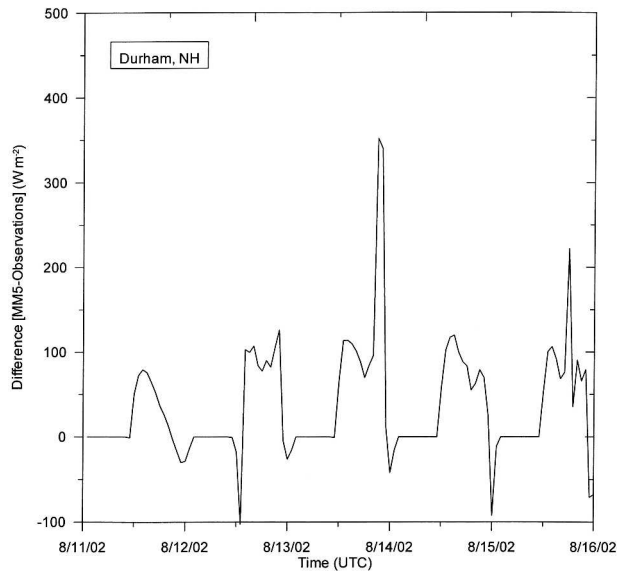


FIG. 5. Difference plot (MM5 – Observations) for Durham, NH, as a function of time for 11–16 Aug 2002.

There is some correlation between the aerosol optical depth and the Eta Model irradiance that can be attributed to increases in the model column water vapor amount and the fact that the aerosols are most likely hygroscopic. The bias in the Eta irradiance estimates at zenith angles of 41° averages 87 W m^{-2} . A prior evaluation of the Eta Model irradiance forecasts under both cloudy and clear-sky conditions found an excess of 50 W m^{-2} (Hinkelman et al. 1999) in the forecast solar irradiance. The MM5 forecast irradiances at 41° show a slightly larger bias of 99 W m^{-2} (Fig. 9).

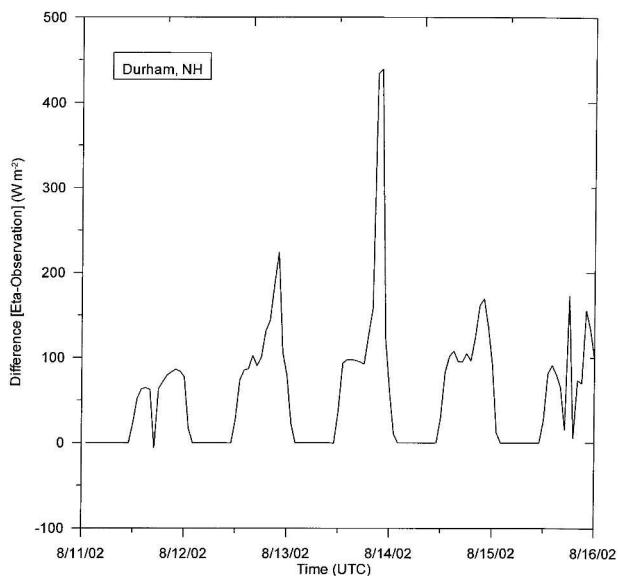


FIG. 6. Difference plot (Eta – Observations) for Durham, NH, as a function of time for 11–16 Aug 2002.

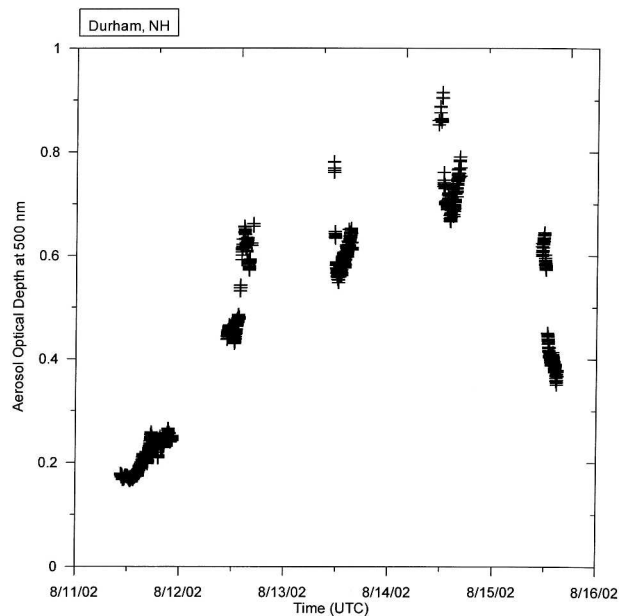


FIG. 7. AODs at 500 nm as a function of time observed at Durham, NH, 11–16 Aug 2002.

The aerosol loading found over Durham, New Hampshire, during NEAQS 2002 resembles the aerosol loading observed over Nashville, Tennessee, during the elevated surface ozone events of SOS 95 and SOS 99 (Zamora et al. 2003). Hybrid Single-Particle Lagrangian Integrated Trajectory (HY-SPLIT) (Draxler 1992) back trajectories computed for the NEAQS 2002 ozone event (not shown) at 500, 1000, and 1500 m indicate that the air passed over the Midwestern states of Ohio, Kentucky, and West Virginia before making its way over Durham. The connection between the sulfate aerosols observed over the northeastern United States and SO_2 emissions from Tennessee and the Ohio Valley has been well established (Dutkiewicz et al. 2000; Malm et al. 2002). Furthermore, recent research results from the Tropospheric Aerosol Radiative Forcing Observational Experiment (TARFOX) and NEAQS (Quinn and Bates 2003) find that in addition to sulfate a significant part of the aerosol distribution can be traced to organics.

Thus, the back trajectories imply that urban/industrial sources are responsible for the Durham elevated optical depths. In contrast, the Houston and Pleasant Grove locations are not regions of the country that are climatologically impacted by high aerosol content. Additionally, diurnal intrusions of marine air from the Gulf of Mexico and Pacific Ocean typically transport cleaner marine air into the northern Central Valley of California and the Gulf Coast.

We suggest that the radiative performance of Lacis and Hansen (1974)-type solar irradiance parameterizations should be adequate for regions of the country not impacted by high aerosol loading, such as the northern

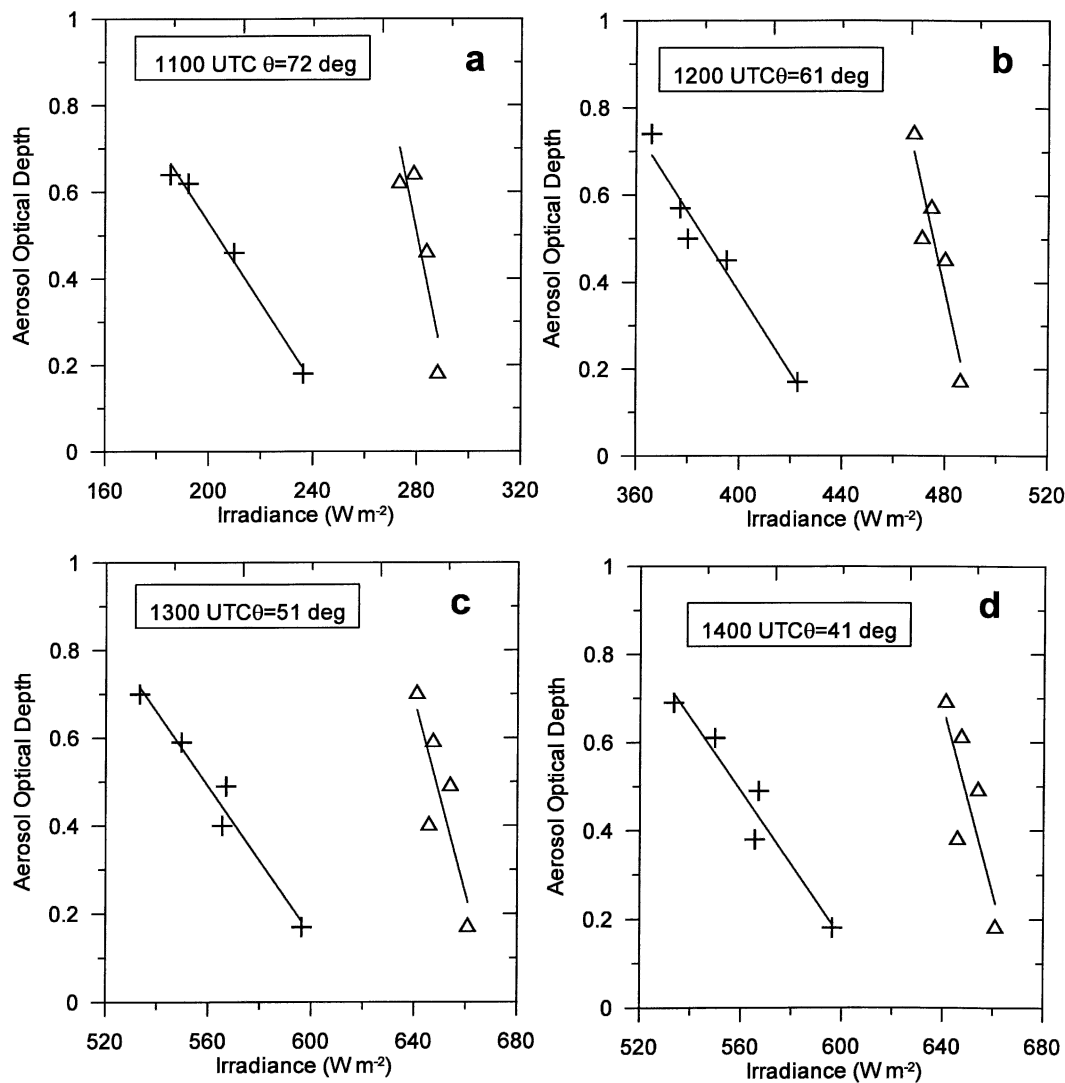


FIG. 8. Correlation between AODs and the observed (crosses) and Eta modeled (triangles) irradiances for (a) 72.0° , (b) 61.0° , (c) 51.0° , and (d) 41.0° zenith angles at Durham, NH, for 11–16 Aug 2002.

Central Valley of California and the Gulf Coast. The observational results of Husar et al. (1997) suggest geographical regions where more sophisticated radiative transfer parameterizations will be needed to achieve accuracy better than $80\text{--}100 W m^{-2}$.

5. Sensitivity tests

We have established that there are situations where errors of $80 W m^{-2}$ are possible in mesoscale model forecasts of solar irradiance. How do these errors impact the surface energy balance in the model, and ultimately how do they affect the skin temperature forecast? Ideally, one should address the sensitivity of the skin temperature forecasts to changes in solar input by running control simulations and perturbed simulations using both MM5 and the Eta Model.

However, the work of Zamora et al. (2003) and Hinkelman et al. (1999) found that compensating errors in the physical parameterizations of the surface energy balance in both MM5 and the Eta Model made isolating the effect of the increased solar irradiance on the MM5 and Eta simulations difficult. In the case of the MM5 simulations, excessively large values of soil moisture evaporation led to $275 W m^{-2}$ errors in the surface latent heat fluxes (Zamora et al. 2003). Presumably, some of the anomalous solar input moistened the surface layer instead of raising the surface layer temperature. Hinkelman et al. (1999) found that the introduction of excess solar radiation in the Eta Model runs did not cause a bias in the daily predicted surface (2 m) temperatures. They concluded that the excess incoming solar radiation must be compensated for by errors elsewhere in the simulated energy budget.

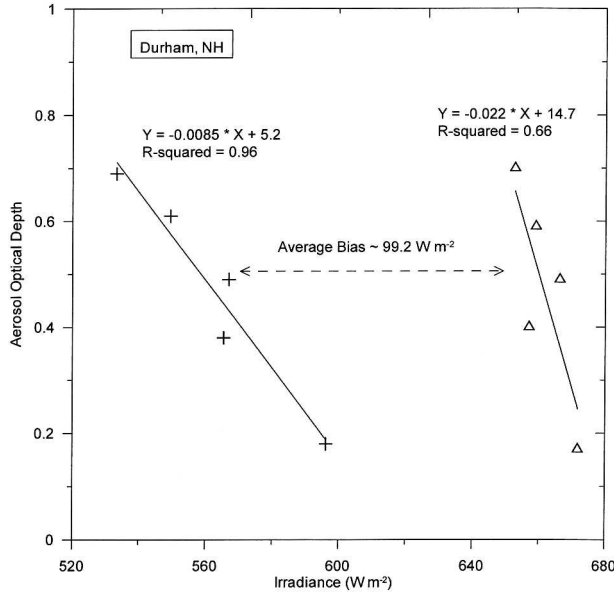


FIG. 9. Correlation between AODs and the observed (crosses) and MM5 modeled (triangles) irradiances for 41.0° zenith angles at Durham, NH, for 11–16 Aug 2002.

Finally, the work of Zhang and Zheng (2004) demonstrates that surface temperature forecasts are very sensitive to the level of closure used in the PBL parameterizations. Given the suggestion that compensating errors are present in the methods used to estimate the surface energy balance in both mesoscale models we addressed the skin temperature sensitivity question using analytic methods and observations of latent and sensible heat fluxes made during elevated ozone events.

The skin temperature forecast in typical mesoscale modeling applications requires numerically solving a form of the following differential equation:

$$C_g \frac{\partial T_g}{\partial t} = R_{\text{net}} - H_s - H_l - K_m C_g (T_g - T_m), \quad (1)$$

where T_g is the skin temperature, t the time, R_{net} the net radiative flux, H_s the sensible heat flux, H_l the latent heat flux, K_m the coefficient of heat transfer from the ground into the substrate, C_g the thermal capacity of the slab per unit area, and T_m the substrate temperature.

The form used here follows that of the Blackadar “Slab” model (Blackadar 1979; Zhang and Anthes 1982). More sophisticated LSMs are now used in MM5 and in the Eta Model. However, this simple model captures the essential physics of a diurnally forced land surface.

Based on flux observations obtained during clear-sky conditions during SOS 99, CCOS 2000, and TexAQ5 2000, we find that the an accurate analytic fit for the time-varying net radiative, latent, and sensible heat fluxes can be cast in the form,

$$F_{\text{rls}}(t) = A_{\text{rls}} \sin^4\left(\frac{\pi t}{\tau}\right) + C_{\text{rls}}, \quad (2)$$

where F_{rls} is the radiative, latent, or sensible heat flux, A_{rls} is the peak flux value, t the time, τ the length of the day, and C_{rls} an offset that can be negative in the case of the net radiative and sensible heat flux, and positive to account for nighttime moisture diffusion when representing the latent heat flux.

Substitution of the analytic forms for the fluxes and rearranging gives

$$\frac{\partial T_g}{\partial t} + K_m T_g = \alpha \sin^4\left(\frac{\pi t}{\tau}\right) + \beta, \quad (3)$$

where $\alpha = (A_r + A_l + A_s)/C_g$, and $\beta = [(C_r + C_l + C_s)/C_g] + K_m T_m$. Equation (3) is linear in time and can be solved in closed form as long as the product of the integrating factor and the right-hand side of (3) can be integrated in terms of elementary functions. The general solution of this differential equation for an initial temperature T_0 is given by

$$T_g(t) = -D - E \cos\left(\frac{2\pi t}{\tau}\right) - F \sin\left(\frac{2\pi t}{\tau}\right) - G \cos\left(\frac{4\pi t}{\tau}\right) - H \sin\left(\frac{4\pi t}{\tau}\right) - K \exp(-K_m t), \quad (4)$$

with

$$D = \frac{3\alpha + 8\beta}{8K_m},$$

$$E = \frac{\alpha K_m \tau^2}{8\pi^2 + 2K_m^2 \tau^2},$$

$$F = \frac{\alpha \pi \tau}{4\pi^2 + K_m^2 \tau^2},$$

$$G = -\frac{\alpha K_m \tau^2}{32\pi^2 + 8K_m^2 \tau^2},$$

$$H = -\frac{\alpha \pi \tau}{32\pi^2 + 2K_m^2 \tau^2},$$

and

$$K = \frac{\tau^4(-T_0 K_m^5 + \beta K_m^4) + 20\tau^2 \pi^2(-K_m^3 T_0 + \beta K_m^2) + 64\pi^4(-T_0 K_m + \beta) + 24\alpha \pi^4}{K_m(K_m^4 \tau^4 + 20K_m^2 \tau^2 \pi^2 + 64\pi^4)}.$$

From the observations, we obtained representative peak flux values for the net radiative, sensible, and latent heat fluxes of 700, 100, and 50 W m^{-2} , respectively. We used offsets of -30 , -40 , and 5 W m^{-2} . The solution of (3) for an initial skin temperature of 304 K, with a substrate temperature of 299 K, $C_g = 9.0 \times 10^5 \text{ J m}^{-2} \text{ K}^{-1}$, $K_m = 3.64 \times 10^{-5} \text{ s}^{-1}$, $\tau = 86400 \text{ s}$, $a = 550 \text{ W m}^{-2}$, and $c = 5 \text{ W m}^{-2}$ is given by

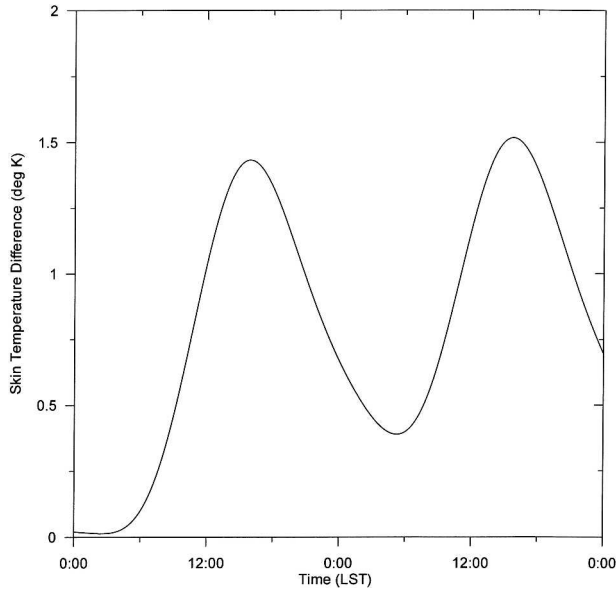


FIG. 10. Skin temperature difference (K) as a function of time.

$$T_g(t) = d - e \cos\left(\frac{2\pi t}{\tau}\right) - f \sin\left(\frac{2\pi t}{\tau}\right) + g \cos\left(\frac{4\pi t}{\tau}\right) + h \sin\left(\frac{4\pi t}{\tau}\right) + k \exp(-K_m t), \quad (5)$$

with $d = 305.45$, $e = 1.68$, $f = 3.36$, $g = 0.12$, $h = 0.49$, and $k = 0.11$.

We then recomputed the solution assuming an 80 W m^{-2} change in the peak net radiative flux. The difference between the two solutions (Fig. 10) indicates that model skin temperature errors of 1.5 K are a possibility given the model error in the net irradiance. This result should be viewed with caution. The solution we show is a linear solution obtained by varying the surface fluxes in time but not allowing them to be a function of skin temperature. We suggest that this solution is most likely the maximum skin temperature perturbation one could anticipate given a Bowen ratio of 2.0 and an 80 W m^{-2} error in solar irradiance. For Bowen ratios smaller than 1.0, we speculate that increases in solar irradiance cause errors in the mean boundary layer mixing ratios rather than skin temperature.

6. Summary and conclusions

Our evaluations of the observed solar irradiance and the forecasts of solar irradiance using parameterizations based on the method of Lacis and Hansen (1974) indicates that the method provides estimates of the solar irradiance that are accurate within 3%–4% as long as the AODs are less than or equal to 0.1. Figure 11 presents a schematic that contrasts clear-sky radiative

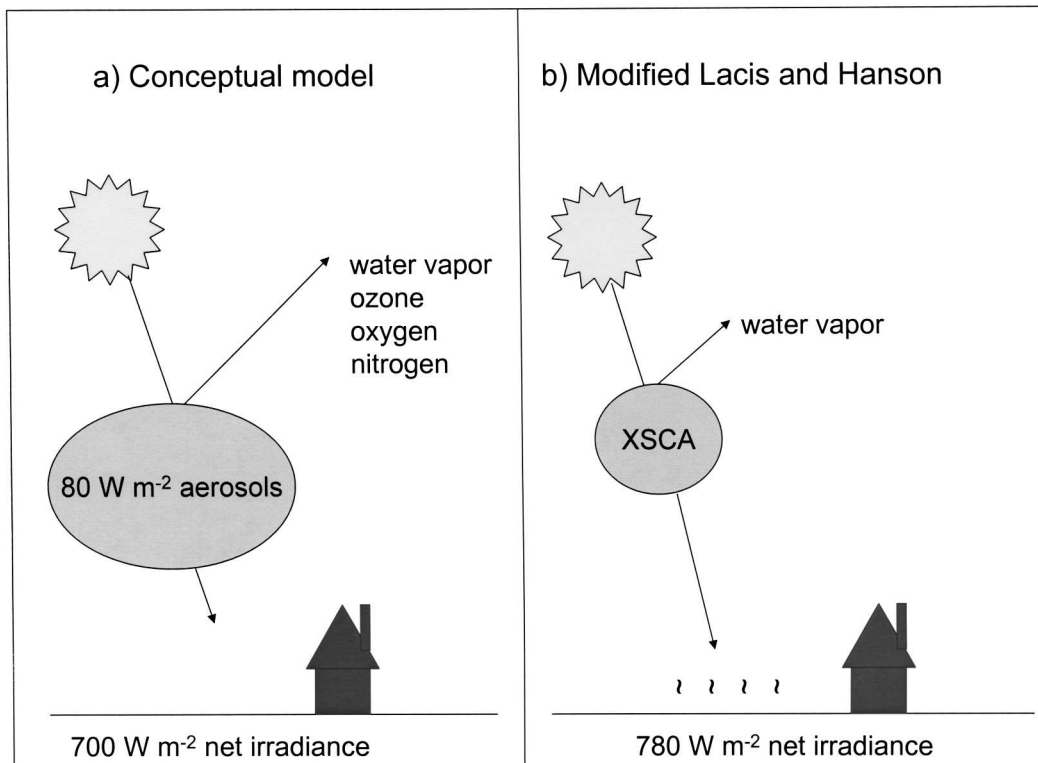


FIG. 11. A schematic summary that illustrates the difference between our conceptual model of atmospheric solar radiative processes in aerosol loaded air masses and their MM5 D89 model counterpart.

processes with their representation using the D89 solar parameterization. Our work suggests that mesoscale forecast models should have few problems simulating clear-sky solar irradiance over the Gulf Coast and the northern Central Valley of California as long as these regions are not affected by long-range transport of aerosols.

During the NEAQS 2002 case study, the AODs exceeded 0.1 on each day of the elevated ozone event. Under these conditions, we found average biases between the Eta and MM5 D89 modeled solar irradiances and the observations of 87.5 and 99.2 W m⁻², respectively. The MM5 result for the NEAQS 2002 case agrees with results obtained by Zamora et al. (2003) during the Nashville SOS 99 and 95 experiments. This work suggests solar irradiance estimates obtained using the default configurations of the MM5 D89 and Eta parameterizations can be in error if the air mass over the region of interest contains significant aerosol loading. The importance of in situ aerosol depth measurements in the assessment of direct radiative forcing in these air masses cannot be overstated.

Using a simple LSM, we have shown that an 80 W m⁻² error in the clear-sky net irradiance can result in a 1.5-K model forecast skin temperature error. This value suggests that clear-sky solar irradiance errors can have a significant impact on numerical model performance.

The next-generation mesoscale forecast models currently being tested are the mass-coordinate and height-coordinate Weather Research and Forecasting (WRF) models. The mass coordinate WRF model incorporates the D89 solar parameterization. Thus, we expect that the results shown in this paper are relevant to mass-coordinate WRF model performance. New studies planned by ETL include the evaluation of the irradiance estimates produced by both WRF models and the NCEP Global Forecast System (GFS) model.

Future research should address the inclusion of prognostic equations for aerosols and the assimilation of ground-based and satellite aerosol optical depth measurements into the forecast models. The MM5, Eta, and WRF modeling systems are used as drivers for air-chemistry models. Improving the aerosol physics in the driving models should improve the performance of the air-chemistry models in regions subject to high aerosol loading. Our findings also suggest that ozone production rates can be impacted by the decreases in solar irradiance presented in this work.

Acknowledgments. The authors wish to thank James Wendell and Donald Nelson (NOAA/CMDL) for their support in the operation of the sun photometer during NEAQS 2002. Bob Weber, Graham Feingold, Christopher Fairall (NOAA/ETL), Donald Nelson, and the anonymous reviewers provided us with timely and thoughtful reviews of the manuscript. This work was supported by the NOAA Health of the Atmosphere

program, the California Air Resources Board, and the Texas Commission on Environmental Quality.

REFERENCES

- Black, T. L., 1994: The new NMC mesoscale Eta Model: Description and forecast examples. *Wea. Forecasting*, **9**, 265–279.
- Blackadar, A. K., 1979: High resolution models of the planetary boundary layer. *Adv. Environ. Sci. Eng.*, **1**, 50–85.
- Burk, S., and W. Thompson, 1989: A vertically nested regional numerical weather prediction model with second order closure physics. *Mon. Wea. Rev.*, **117**, 2305–2324.
- Draxler, R. R., 1992: Hybrid Single-Particle Lagrangian Integrated Trajectories (HY-SPLIT): Version 3.0: Users guide and model description. Tech. Rep. ERL ARL-195, NOAA, Silver Spring, MD, 28 pp.
- Dudhia, J., 1989: Numerical study of convection observed during the Winter Monsoon Experiment. *J. Atmos. Sci.*, **46**, 118–133.
- Dutkiewicz, V. A., M. Das, and L. Husain, 2000: The relationship between regional SO₂ emissions and downwind aerosol sulfate concentrations in the northeastern US. *Atmos. Environ.*, **34**, 1821–1832.
- Dutton, E. G., J. J. Michalsky, T. Stoffel, B. W. Forgan, J. Hickey, D. W. Nelson, T. L. Alberta, and I. Reda, 2001: Measurement of broadband diffuse solar irradiance using current commercial instrumentation with a correction for thermal offset errors. *J. Atmos. Oceanic Technol.*, **18**, 297–314.
- Grell, G. A., 1993: Prognostic evaluation of assumptions used by cumulus parameterizations. *Mon. Wea. Rev.*, **121**, 764–787.
- , J. Dudhia, and D. R. Stauffer, 1994: A description of the fifth-generation Penn State/NCAR Mesoscale Model (MM5). Tech. Note NCAR/TN-398+IA, National Center for Atmospheric Research, Boulder, CO, 122 pp.
- , S. Emeis, W. R. Stockwell, T. Schoenemeyer, R. Forkel, J. Michalakes, R. Knoche, and W. Seidel, 2000: Application of a multiscale, coupled MM5/chemistry model to the complex terrain of the VOLTAP valley campaign. *Atmos. Environ.*, **28**, 1435–1453.
- Guichard, F., D. B. Parsons, J. Dudhia, and J. Bresch, 2003: Evaluating mesoscale model predictions of clouds and radiation with SGP ARM data over a seasonal timescale. *Mon. Wea. Rev.*, **131**, 926–944.
- Hinkelman, L. M., T. P. Ackerman, and R. T. Marchand, 1999: An evaluation of NCEP Eta Model predictions of surface energy budget and cloud properties by comparison with measured ARM data. *J. Geophys. Res.*, **104** (D16), 19 535–19 549.
- Husar, R. B., J. M. Prospero, and L. L. Stowe, 1997: Characterization of tropospheric aerosols over the ocean with the NOAA Advanced Very High Resolution Radiometer optical thickness operational product. *J. Geophys. Res.*, **102** (D14), 16 889–16 909.
- Janjic, Z. I., 1997: The step-mountain coordinate model: Further developments of the convection, viscous sublayer, and turbulence closure schemes. *Mon. Wea. Rev.*, **122**, 927–945.
- Lacis, A. A., and J. E. Hansen, 1974: A parameterization for the absorption of solar radiation in the earth's atmosphere. *J. Atmos. Sci.*, **31**, 3077–3107.
- Malm, W. C., B. A. Schichtel, R. B. Ames, and K. A. Gebhart, 2002: A 10-year spatial and temporal trend of sulfate across the United States. *J. Geophys. Res.*, **107**, 4627, doi:10.1029/2002JD002107.
- Philipona, R., 2002: Underestimation of solar global and diffuse radiation measured at the earth's surface. *J. Geophys. Res.*, **107**, 4645, doi:10.1029/2002JD002396.
- Quinn, P. K., and T. S. Bates, 2003: North American, Asian, and Indian haze: Similar regional impacts on climate? *Geophys. Res. Lett.*, **30**, 1555, doi:10.1029/2003GL016934.
- Rogers, E., T. L. Black, D. G. Deaven, G. J. Dimego, Q. Zhao, M. Baldwin, N. W. Junker, and Y. Lin, 1996: Changes to the operational “early” Eta analysis/forecast system at the Na-

- tional Centers for Environmental Prediction. *Wea. Forecasting*, **11**, 391–413.
- Satheesh, S. K., V. Ramanathan, X. Li-Jones, J. M. Lobert, I. A. Podgorny, J. M. Prospero, B. N. Holben, and N. G. Loeb, 1999: A model for the natural and anthropogenic aerosols over the tropical Indian Ocean derived from the Indian Ocean Experiment data. *J. Geophys. Res.*, **104**, 27 421–27 440.
- Seaman, N. L., and S. A. Michelson, 2000: Mesoscale meteorological structure of a high-ozone episode during the 1995 NARSTO-Northeast study. *J. Appl. Meteor.*, **39**, 384–398.
- Smirnova, T. G., J. M. Brown, and S. G. Benjamin, 1997: Performance of different soil model configurations in simulating ground surface temperature and surface fluxes. *Mon. Wea. Rev.*, **125**, 1870–1884.
- Zamora, R. J., and Coauthors, 2003: Comparing MM5 radiative fluxes with observations gathered during the 1995 and 1999 Nashville southern oxidants studies. *J. Geophys. Res.*, **108**, 4050, doi:10.1029/2002JD002122.
- Zhang, D., and R. A. Anthes, 1982: A high-resolution model of the planetary boundary layer-sensitivity tests and comparisons with the SESAME-79 data. *J. Appl. Meteor.*, **21**, 1594–1609.
- , and W.-Z. Zheng, 2004: Diurnal cycles of winds and temperatures as simulated by five boundary layer parameterizations. *J. Appl. Meteor.*, **43**, 157–169.